AD-A126 828 EXPERIMENTAL AND THEORETICAL INVESTIGATION OF MICROWAVE AND MILLIMETER WA..(U) MARYLAND UNIV COLLEGE PARK DEPT OF ELECTRICAL ENGINEERING W W DESTLER ET AL. NOV 82 1/1

UNCLASSIFIED AFOSR-TR-83-0201 AFOSR-78-3690 F/G 20/7 NL

END
DATE FILMED
5-83
DTIC

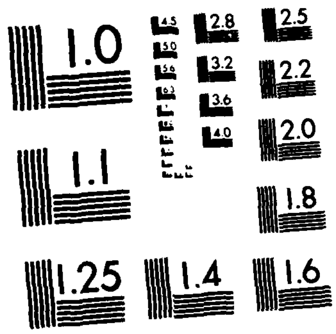


MICROCOPY RESOLUTION TEST CHART
NATIONAL BUREAU OF STANDARDS-1963-A

EXPERIMENTAL AND THEORETICAL INVESTIGATION OF MICROWAVE AND MILLIMETER WAVE RADIATION FROM HOLLOW, ROTATING, ELECTRONS BEAMS

Contract No. AFOSR-78-3690

PROGRESS REPORT

For the Period December 1, 1981 through November 30, 1982



Submitted to

Air Force Office of Scientific Research

Prepared by

Charged Particle Beam Research Group
Electrical Engineering Department
University of Maryland
College Park, Maryland 20742

UNCLASSIFIED
SECURITY CLASSIFICATION OF THIS PAGE (When Data Entered)

# REPORT DOCUMENTATION PAGE

READ INSTRUCTIONS BEFORE COMPLETING FORM

| | |
|---|---|
| 1. REPORT NUMBER AFOSR-TR- 83-0201 | 2. GOVT ACCESSION NO. A126828 |
| 3. RECIPIENT'S CATALOG NUMBER | |
| 4. TITLE (and Subtitle) EXPERIMENTAL AND THEORETICAL INVESTIGATION OF MICROWAVE AND MILLIMETER WAVE RADIATION FROM HOLLOW, ROTATING, ELECTRON BEAMS | 5. TYPE OF REPORT & PERIOD COVERED Annual 1 Dec 81 - 30 Nov 82 |
| | 6. PERFORMING ORG. REPORT NUMBER |
| 7. AUTHOR(s) William W. Destler, Charles D. Striffler, Won Namkung | 8. CONTRACT OR GRANT NUMBER(s) AFOSR-78-3690 |
| 9. PERFORMING ORGANIZATION NAME AND ADDRESS University of Maryland Electrical Engineering Department College Park, MD 20742 | 10. PROGRAM ELEMENT, PROJECT, TASK AREA & WORK UNIT NUMBERS 61102F 2301/A8 |
| 11. CONTROLLING OFFICE NAME AND ADDRESS AFOSR/NP Bolling AFB, Bldg. # 410 Washington DC 20332 | 12. REPORT DATE Nov 1982 |
| | 13. NUMBER OF PAGES 22 |
| 14. MONITORING AGENCY NAME & ADDRESS (if different from Controlling Office) | 15. SECURITY CLASS. (of this report) Unclassified |
| | 15a. DECLASSIFICATION DOWNGRADING SCHEDULE |

16. DISTRIBUTION STATEMENT (of this Report)

Approved for public release; distribution unlimited

17. DISTRIBUTION STATEMENT (of the abstract entered in Block 20, if different from Report)

18. SUPPLEMENTARY NOTES

19. KEY WORDS (Continue on reverse side if necessary and identify by block number)

20. ABSTRACT (Continue on reverse side if necessary and identify by block number)

The technical summary is divided into three parts, one describing the equipment status, the second the experimental program, and the third outlines the theoretical studies that have been initiated. A list of publications and presentations resulting from this work may be found in the Appendix.

DD FORM 1 JAN 73 1473

UNCLASSIFIED
SECURITY CLASSIFICATION OF THIS PAGE (When Data Entered)

# EXPERIMENTAL AND THEORETICAL INVESTIGATION OF MICROWAVE AND MILLIMETER WAVE RADIATION FROM HOLLOW, ROTATING, ELECTRON BEAMS

Contract No. AFOSR-78-3690

PROGRESS REPORT

For the Period December 1, 1981 through November 30, 1982

Submitted to

Air Force Office of Scientific Research



Prepared by

Charged Particle Beam Research Group
Electrical Engineering Department
University of Maryland
College Park, Maryland 20742

PROGRESS REPORT

| | |
|---|---|
| SUBMITTED TO: | Air Force Office of Scientific Research |
| SUBMITTED BY: | Electrical Engineering Department<br>University of Maryland<br>College Park, MD 20742 |
| GRANT NUMBER: | AFOSR-78-3690D |
| AMOUNT: | $102,083 |
| PERIOD: | December 1, 1981 to November 30, 1982 |
| PRINCIPAL INVESTIGATORS: | William W. Destler, Associate Professor<br>Charles D. Striffler, Associate Professor<br>Won Namkung, Assistant Professor<br>Electrical Engineering Department |
| TITLE OF RESEARCH PROJECT: | "Experimental and Theoretical Investigation of Microwave Radiation from Hollow, Rotating, Electron Beams" |

# INTERIM PROGRESS REPORT

for the Period December 1, 1981, to November 30, 1982

## I. Introduction

The technical summary is divided into three parts, one describing the equipment status, the second the experimental program, and the third outlines the theoretical studies that have been initiated. A list of publications and presentations resulting from this work may be found in the Appendix.

## II. Experimental Apparatus and Equipment

During the summer of 1981, the Charged Particle Beam Laboratory, including all of the facilities used for this research, was moved into the new Energy Research Building on the University of Maryland campus. As a result, our group now shares facilities with the plasma physics program, and the close interaction between our groups will undoubtedly strengthen our research. More importantly, however, we now have ample space for our experimental facilities in a modern, well designed research building. Relocation of our electron accelerator, cusp magnetic field system, microwave diagnostics, and associated facilities was a major job. Normal operation of the Laboratory was resumed in October, 1981.

A second electron beam generator, called Dragon, built in collaboration with researchers at the Harry Diamond Laboratory, has been constructed and is undergoing initial high voltage testing. Dragon has a lower voltage (1 MV), but higher current (150 kA maximum, variable using a special output shunt resistor) and longer pulse length (100 ns) than our existing accelerator (2 MV, 30 kA, 30 ns). This new facility will eventually allow us to perform scaling experiments at electron energies between the present work and the Cusptron experiment, currently under construction.

The table top rotating beam experiment, Cusptron, is in the early stages of construction, with many components either on hand or on order. Design details of this experiment have been finalized and are summarized in the next section.

## III. Experimental Research

Despite the shortened work year caused by the relocation of our laboratory, significant experimental studies have been conducted. These include:

1) Studies of the radiation produced when a 6.0 cm radius rotating E-layer interacts with a smooth 7.0 cm outer conducting boundary (with and without inner conductors) were conducted and the results compared with previous results obtained using a 7.5 cm outer conducting boundary. Theoretical predictions that the peak in the radiated power should move up in frequency to Ku band (12-18 GHz) were confirmed. Radiation was broadband, as expected, and peak powers in Ku band comparable to those achieved in X-band using the 7.5 cm tube were measured. Detailed analysis of this data is not yet complete.

2) The impressive results obtained during the previous contract period when a rotating beam was injected into a 12 cavity magnetron-type outer conducting boundary have prompted a systematic study aimed at optimizing radiation production at the $20^{th}$ harmonic of the cyclotron frequency. This value was chosen because $20\ \omega_{ce}$ corresponds to about 16 GHz, a value in the center of Ku band, where detection equipment is available. Theoretical work supporting this effort is discussed in the next section. Because outer magnetron conducting boundaries are difficult to construct to the tolerances required for operation at this frequency, it was decided that slotted inner conductors would be used to determine the best operating parameters. A schematic of this configuration is shown in Fig. 1a. Such a configuration probably is not the optimum one (outer slotted boundaries should produce higher radiated powers as well as better long pulse operation) but has yielded important insights into the operating characteristics of such systems.

Fig. 2a shows a typical radiated power spectrum in Ku band for an $\ell = 20$ inner magnetron boundary. Radiation is strongly peaked at $20\ \omega_{ce}$, as predicted, indicating the radiation is produced in the "$2\pi$" mode of the boundary system. The total radiated power of about 10 MW is probably an underestimate. In the absence of a Ku band source powerful enough to calibrate our 36 m Ku band dispersive line in place, we have used the theoretical waveguide attenuation values. In reality, the waveguide attenuation is always worse than these values. In light of such difficulties, it is difficult to estimate accurately the efficiency of the system (injected beam energy is about 2 MeV, injected current is in the range 1-2 kA), but it is certainly approaching 1%.

Radiation from a crudely constructed $\ell = 20$ outer magnetron boundary is shown in Fig. 2b. The frequency of operation has dropped to 11 GHz in this case. (The reason for the different operating frequency is not clear, although it is possible that a mode other than the "$2\pi$" is being excited.) Studies of the effect of slot depth and the radius of inner and outer conducting boundaries on the radiation process are currently underway. Preliminary indications are that increasing the slot depth and reducing the distance between the beam and the conducting boundaries both result in higher radiated powers.

3) The results at $\ell = 20$ prompted a quick look at radiation from a third experimental configuration, shown schematically in Fig. 1b. Here both the $\ell = 20$ inner and outer conducting boundaries were employed, with the slots shifted $180^{\circ}$ with respect to each other. A typical radiated power spectrum is shown in Fig. 3. Not surprisingly, the resonance was shifted up into Ka band, with strong peaks at both 26 GHz and 41 GHz. Because waveguide attenuation is quite severe in Ka band, a 6 m length of the 36 m long Ka band dispersive line was calibrated at these frequencies to better estimate the radiated power. (For example, the measured waveguide attenuation at 40 GHz was 1.3 dB/m, compared

to the theoretical value of 1 dB/m.) A detailed understanding of this phenomena awaits further theoretical work, but it is apparent that the beam sees effectively a 40 slot system. In planar geometry such a system is referred to as one with "Glide Reflection Symmetry," and early theoretical analysis has shown that in such systems the effective periodicity of the structure is d/2, where d is the slot period.

4) The Cusptron experiment is in the early stages of construction, with essential components ordered and some of them already on hand. Electron beam parameters remain the same as those in the last report. Design details for the initial experiment have been finalized and are listed in Table 1. A schematic diagram of the planned experimental setup is shown in Fig. 4.

In the area of the electron gun design, we have acquired the computer code developed by W. Herrmannsfeldt at SLAC, and modification of the code for our unique diode geometry is in progress. This code will be used to shape the electrode geometry for maximum diode efficiency.

The major considerations in the design of the experiment are summarized as follows: The dimensions of the emitting surface are determined by considering the fact that the canonical angular momentum spread of the beam is to be minimized and also that there should be enough total emission current to satisfy experimental goals. This dimension fixes the radius of the rotating E-layer in the downstream drift region and also the optimum size of the downstream vacuum chamber from the beam-waveguide mode interaction mechanism. The diode side vacuum chamber should be large enough to prevent electrical breakdown.

## IV. Theoretical Research

Over the past few years we have analyzed in detail the mode structure (dispersion relation) and field profiles in hollow and coaxial cylindrical waveguides. Likewise, the linear stability analysis of a rotating E layer interacting with and transferring energy to these waveguide modes was completed for the appropriate parameter regime of the experiments. In general, we found that such an interaction should generate many unstable harmonic modes leading to what we have called broadband radiation. Both theory and experiment are in good agreement for these beam-waveguide systems.

This past year we have examined two other waveguide geometries, shown in Figs. 5a and 5b and have analyzed the mode structure of each. For the first case, the dielectric lined hollow waveguide whose geometry is shown in Fig. 5a, the results from calculating the dispersion relation are shown in Fig. 6. The fields in general do not decompose into purely TE and TM but are hybrid modes. In Figs. 6a-6c, we have displayed the dispersion relation for the $\ell = 1$ and $\ell = 5$ azimuthal harmonic mode numbers with the radial mode number $n_r$ as a parameter. In Figs. 6a and 6b, the dimensions are $R_d = 7.0$ cm, $R_w = 7.5$ cm, with the dielectric constant $\varepsilon_r = 6.1$. We have drawn for reference the velocity of light lines in vacuum and in the dielectric. In Fig. 6c, the dielectric liner has a radius of 6.5 cm. Also drawn on each graph is the appropriate $\ell\omega_{ce} = \ell(eB_o/m\gamma)$ for a rotating beam of $\gamma = 6$, beam radius $R = 6$ cm, and assuming no axial beam velocity $\omega_{ce} = v_\phi/R = (c/R)(\gamma^2 - 1)^{1/2}/\gamma$. If no dielectric liner is present, there would exist no beam-waveguide mode intersection for either the $\ell = 1$ or $\ell = 5$ harmonic. However, we see that for $\ell = 5$ there is an intersection with the $n_r = 1$ mode for a .5 cm thick liner and with the $n_r = 1$ and 2 radial modes for a 1 cm thick liner. An important point should be noted; that is, intersections of a beam mode and a waveguide mode in the region above the $\omega = k_z c$ line will lead to good coupling, whereas, interactions in the region between the $\omega = k_z c/\sqrt{\varepsilon_r}$ and $\omega = k_z c$ lines does not, because in this latter case most of the field is located in the dielectric and not in the region of the beam. In summary, a dielectric liner reduces the cutoff frequency $\omega_{co}(k_z = 0)$ which is one means of producing beam-waveguide interaction with a low energy beam as in the Cusptron experiment.

For the second case, the <u>magnetron type slotted waveguide</u>, whose geometry is shown in Fig. 5b, the field structure is again of the hybrid type except in the limit of $k_z = 0$, that is, the cutoff limit. In this limit, the interesting mode is the TE mode, since in this case there is an $E_y$ component of the electric field which is in the direction of the beam motion. The field components are $\underset{\sim}{E} = (E_x, E_y, 0)$, $\underset{\sim}{H} = (0, 0, H_z)$ and the dispersion equation is

$$\frac{1}{K_{n'}} \cot K_{n'}\ell + \frac{w}{2d} \sum_{n=-\infty}^{\infty} \frac{1}{K_n} \cot K_n a$$

$$\times \left\{ \frac{\sin^2 \frac{w}{2} (\frac{\pi n'}{w} + k_{yn})}{[\frac{w}{2} (\frac{\pi n'}{w} + k_{yn})]^2} + \frac{\sin^2 \frac{w}{2} (\frac{\pi n'}{w} - k_{yn})}{[\frac{w}{2} (\frac{\pi n'}{w} - k_{yn})]^2} + \right.$$

$$\left. + 2(-1)^{n'} \frac{\sin \frac{w}{2} (\frac{\pi n'}{w} + k_{yn})}{\frac{w}{2} (\frac{\pi n'}{w} + k_{yn})} \frac{\sin \frac{w}{2} (\frac{\pi n'}{w} - k_{yn})}{\frac{w}{2} (\frac{\pi n'}{w} - k_{yn})} \right\} = 0$$

where we assume a given field profile for $E_y$ at the interface between the slot and interaction region, that is, $E_y(0,y) = E_o \cos n'\pi y/w$, $0 < y < w$, by choosing a value for $n' = 0,1,\ldots$ . The other parameters are; $n'$--order of the slot mode, $k_{yn}$--$n^{th}$ harmonic of the traveling wave in the interaction region, $K_{n'}^2 = \omega^2/c^2 - (\pi n'/w)^2$, $K_n^2 = \omega^2/c^2 - k_{yn}^2$, $k_{yn} = k_y + 2\pi n/d$, $k_y d$-- represents the phase shift of $E_y(0,y)$ from slot to slot. Graphical results of this equation for the $n' = 0$ (constant field across the gap) and $n' = 1$ (first harmonic mode) are shown in Figs. 7 and 8 for two different geometries. In Fig. 7, the geometry is chosen to represent a 12 slot cylindrical system and in Fig. 8, the geometry represents a 20 slot system. The specific dimensions are given in each figure caption. We have plotted the first few branches of the solution to the dispersion equation which can be thought of as different x-direction modes (radial mode in the cylindrical system). Again we have drawn the velocity of light line on each graph which also represents approximately our beam mode. The various intersections represent beam-waveguide mode resonant interaction. Our goal is to have the first mode interaction to occur with a $2\pi$ guide mode, which is approximately true for the $n' = 1$ slot mode cases. For the 12 slot case, Fig. 7, we would expect interaction near 10 GHz and for the 20 slot case, Fig. 8, slightly below 20 GHz. A cylindrical version of this geometry is under investigation to more accurately determine the resonant frequencies.

TABLE 1

Principal Parameters of the Cusptron Experiment Design

| | |
|---|---|
| 1. **Electron Gun** | |
| Emitting Surface | 2.8 cm Inner diameter<br>3.2 cm Outer diameter<br>1.89 $cm^2$ Area |
| Anode-Cathode Gap | 5.5-7.0 cm (Adjustable) |
| Anode Aperture | The same as the emitting surface with 4-place supporting bridges |
| 2. **Vacuum Chambers and Pumps** | |
| Diode Chamber | 6" Outer diameter stainless steel with water cooling<br>30 ℓ/s ion pump |
| Downstream Chamber | 4" Outer diameter stainless steel, 60 cm long, 20 ℓ/s ion pump |
| 3. **Magnets and Magnet Power Supplies** | |
| Diode Side | 8" Inner diameter, 15 cm long,<br>NI = 8.8 KAmp-turn<br>Kepco 20 A to 25 V, regulated |
| Downstream Side | 5" Inner diameter, 50 cm long,<br>NI = 30 KAmp-turn<br>Kepco 30 A to 36 V, regulated |
| 4. **Main Power Supplies** | |
| Heater | 0-10 V, 0-10 A ac floating |
| Anode | 2.5 Amp 20 KV for the initial beam test |
| 5. **Beam Diagnostics** | |
| Current Monitor | Rogowski coil after the cusp |
| Beam Shape | Phosphor screens |

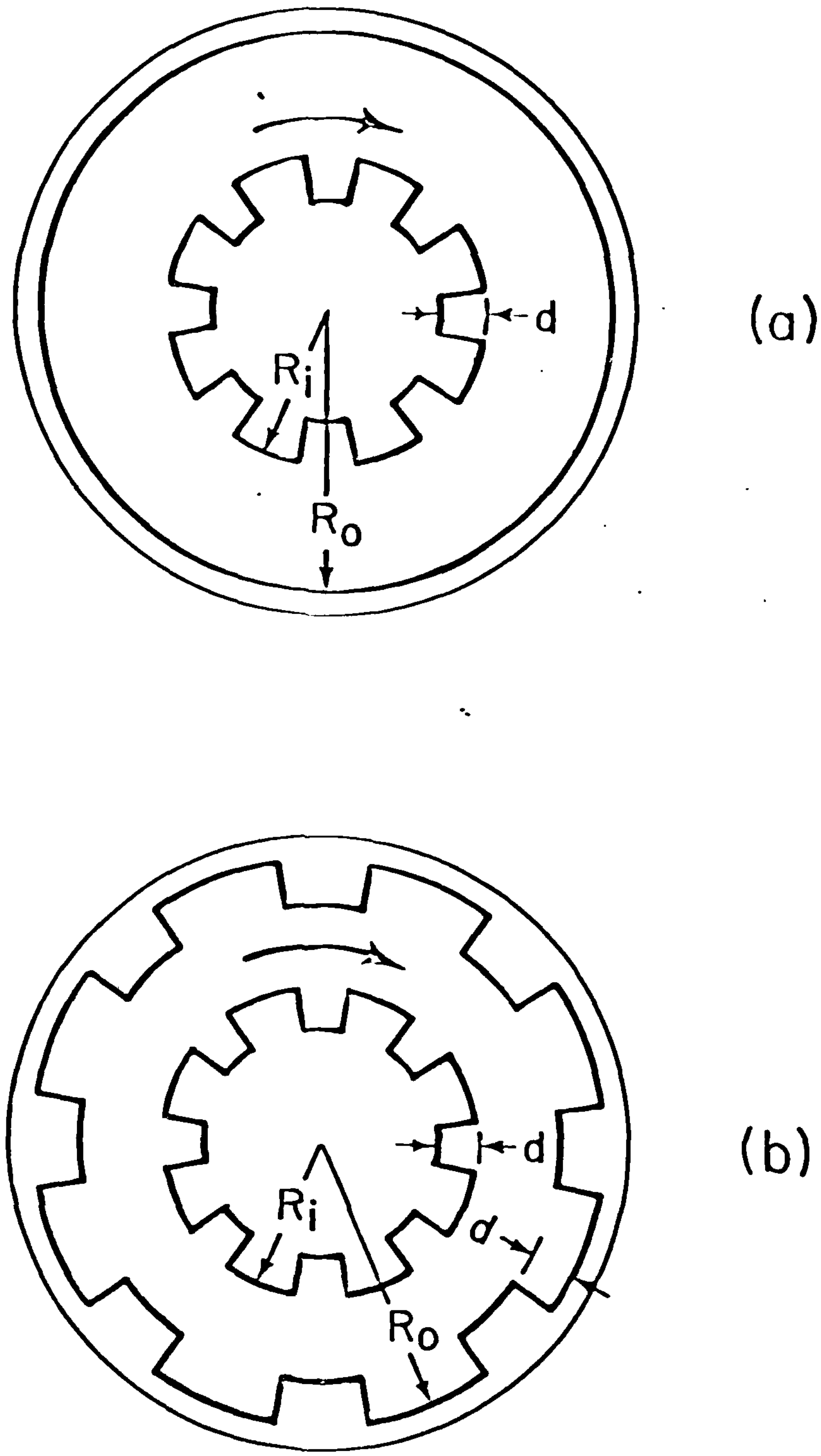


FIG. 1 Schematic of Experimental Magnetron Conducting Boundary Configurations.

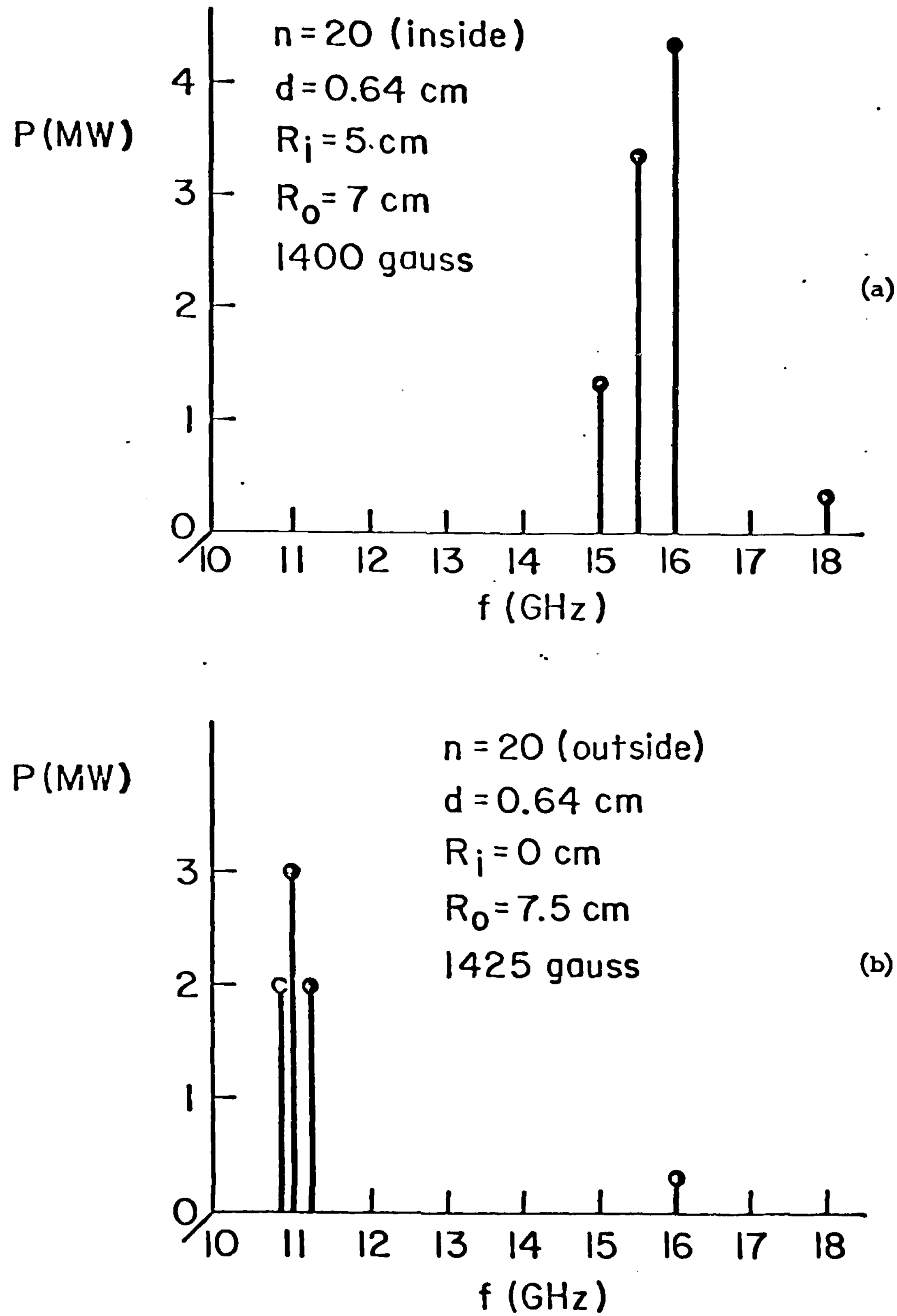


FIG. 2 Radiated Power in Ku-band for (a) an inner $\ell$ = 20 magnetron boundary, and (b) an outer $\ell$ = 20 magnetron boundary.

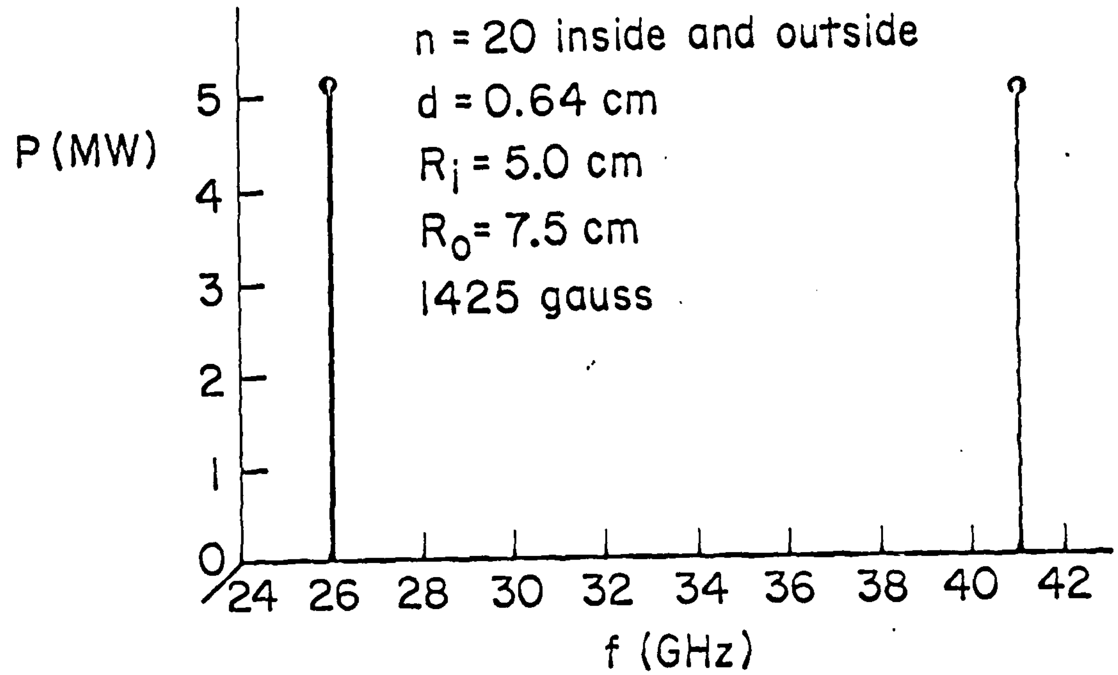


FIG. 3 Radiated Power in Ka-band for an $\ell$ = 20 inner and outer magnetron conducting boundary system configured as shown in Fig. 1b.

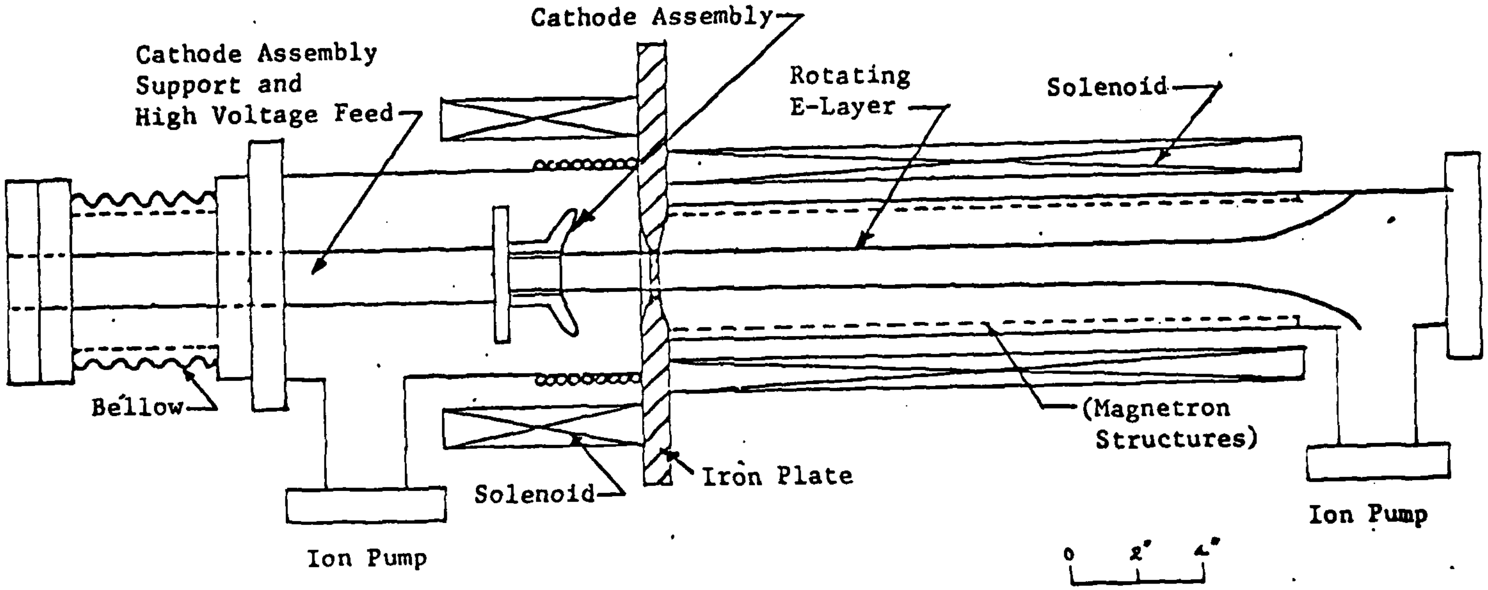


FIG. 4. Schematic Diagram of the CUSPTRON Experiment

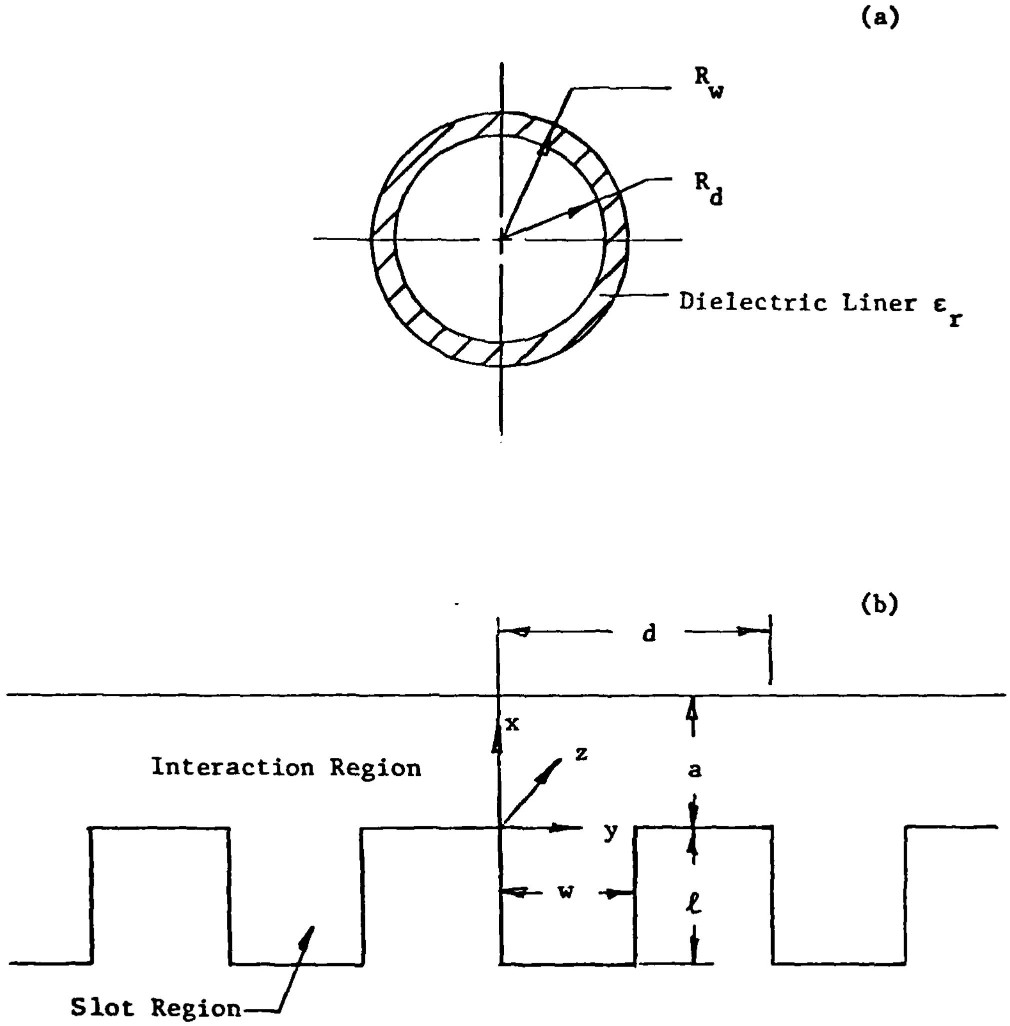


FIG. 5 Waveguide Structures under Investigation:
(a) Dielectric lined-hollow waveguide
(b) Magnetron type slotted waveguide (cartesian model).

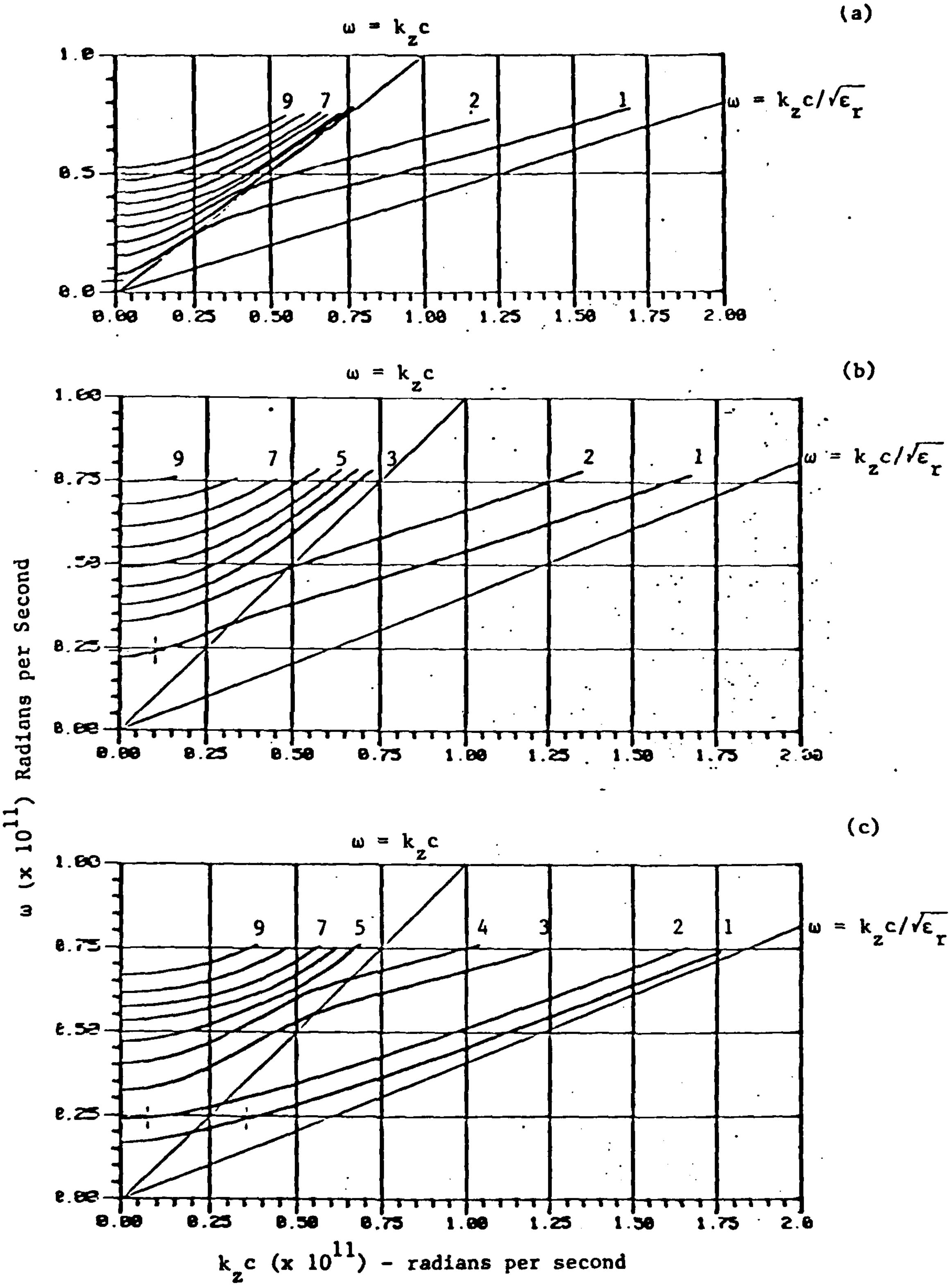


FIG. 6 Dielectric Lined Dispersion Relation, $R_w = 7.5$ cm, $\varepsilon_r = 6.1$;(a) $R_d = 7.0$ cm, $\ell = 1$,(b) $R_d = 7.0$ cm, $\ell = 5$, (c) $R_d = 6.5$ cm, $\ell = 5$. $n_r$ is a parameter. See Fig. 5.

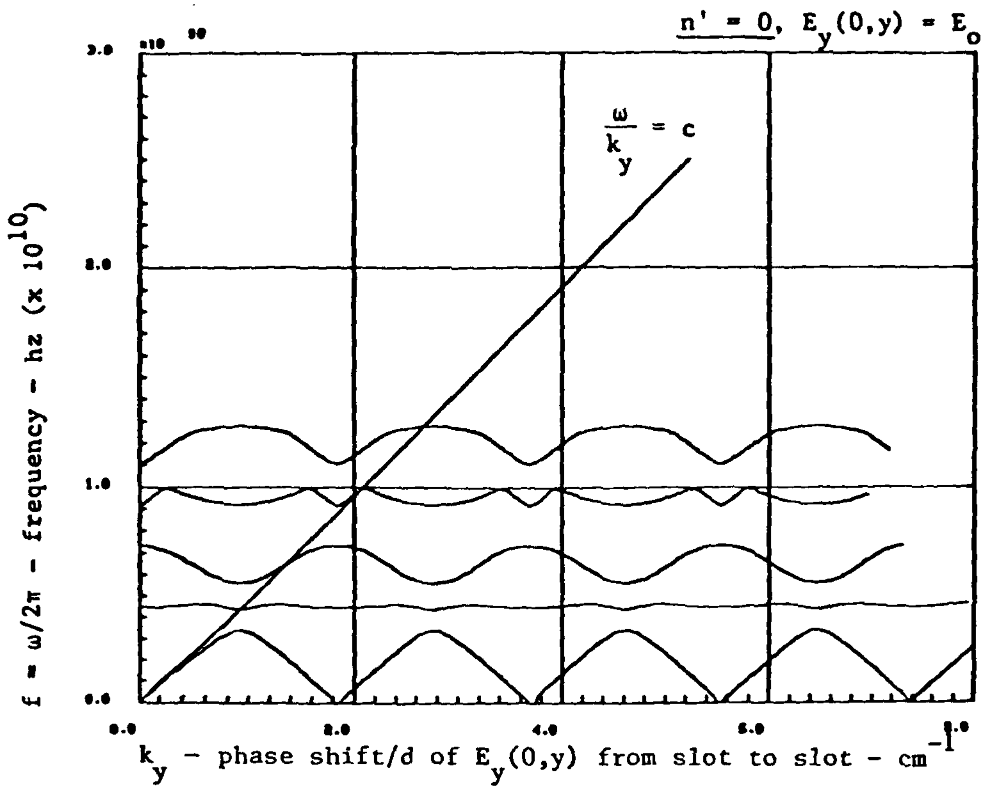


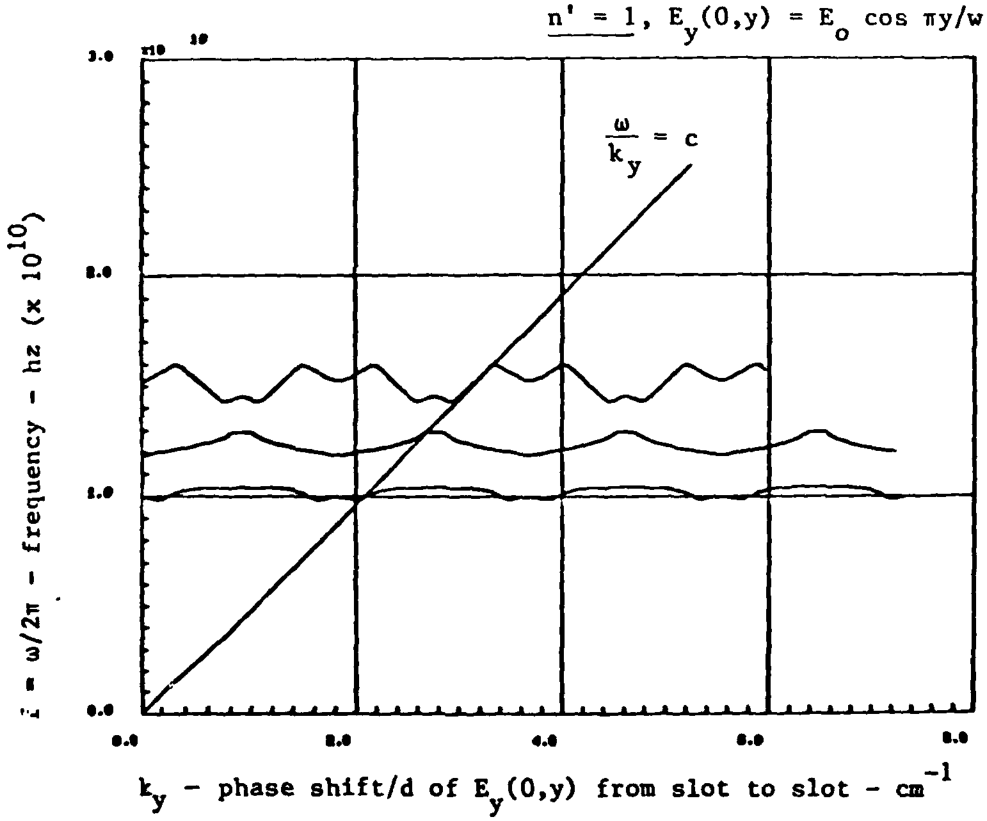


FIG. 7 Dispersion relation for the n' = 0 and 1 slot modes. The geometry is a = 2.5 cm, d = 3.4 cm, w = d/z = 1.7 cm, $\ell$ = 1 cm, and this is equivalent to a 12 slot magnetron outer wall.

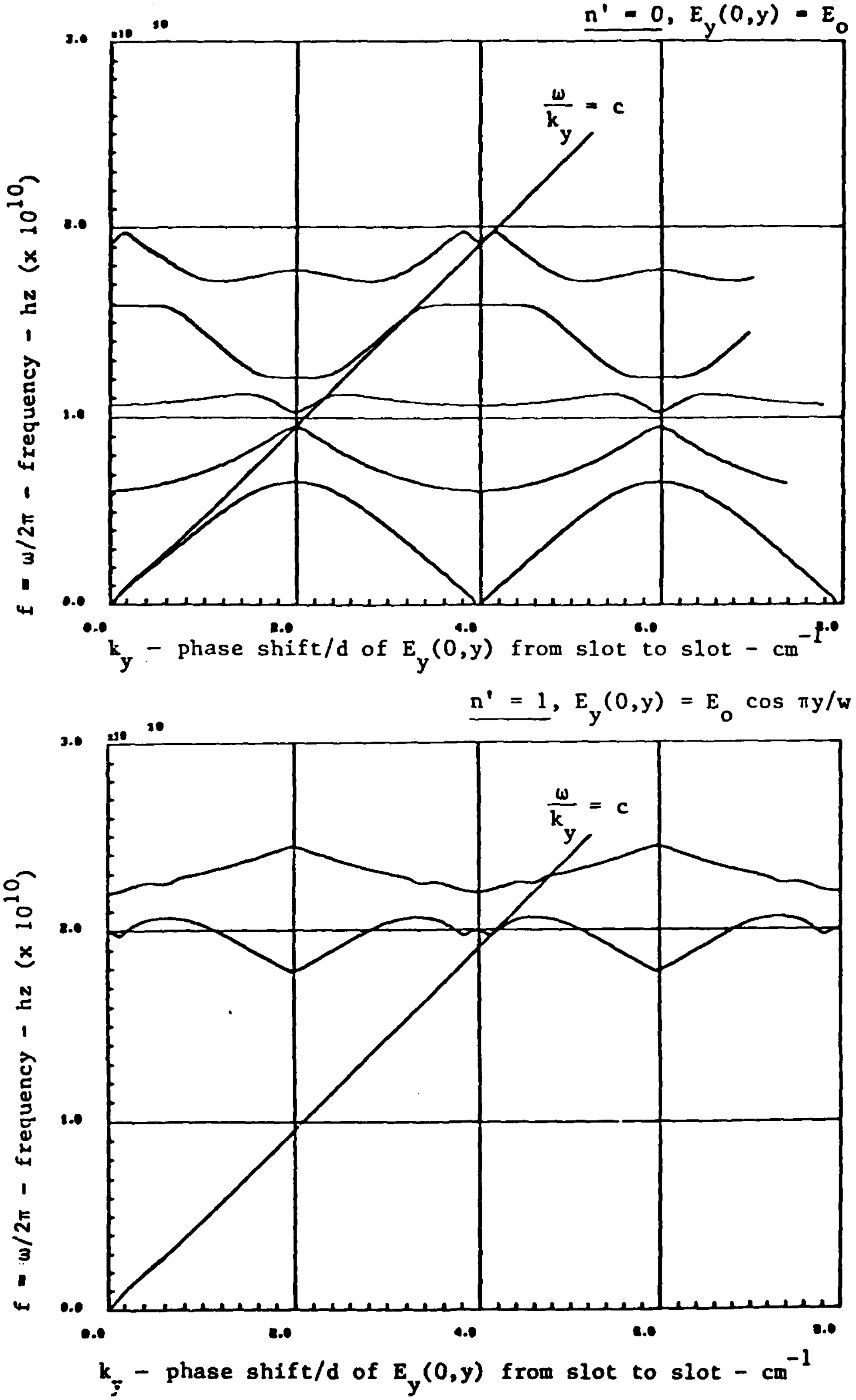


FIG. 8 Dispersion relation for the n' = 0 and 1 slot modes. The geometry is a = 2 cm, d = 1.6 cm, w = d/2 = .8 cm, $\ell$ = .64 cm, and this is equivalent to a 20 slot magnetron inner wall.

# APPENDIX

## List of Publications and Presentations Resulting from this Work

1. "Experimental Study of Intense Microwave Generation by the Negative Mass Instability," W. W. Destler, W. Namkung, and R. L. Weiler, Bull. Am. Phys. Soc. 24, 1068 (October 1979).

2. "Theoretical Study of Microwave Generation from a Rotating E-Layer-Coaxial Waveguide System," W. Namkung, H. Romero, and C. D. Striffler, Bull. Am. Phys. Soc. 24, 1068 (October 1979).

3. "Negative Mass Instability of a Relativistic E Ring in a Hollow Waveguide," T. F. Wang and C. D. Striffler, Bull. Am. Phys. Soc. 24, 1068 (October 1980).

4. "High Power Microwave Generation from an Intense Rotating Electron Beam," W. W. Destler, C. D. Striffler, W. Namkung, H. Romero, and R. Weiler, 1980 IEEE Int. Conf. on Plasma Science, Madison, WI (May 19-21, 1980).

5. "High Power Microwave Generation from a Cusp-Injected Magnetron," W. W. Destler, R. Kulkarni, C. D. Striffler, and R. L. Weiler, Bull. Am. Phys. Soc. II, 25, 886 (1981).

6. "High Power Microwave Generation from a Rotating E-Layer in a Magnetron-Type Waveguide," W. W. Destler, R. L. Weiler, and C. D. Striffler, Appl. Phys. Lett. 38, 570 (1981).

7. "High Power Microwave Generation from a Rotating E-Layer in Various Conducting Wall Systems," W. W. Destler, R. Kulkarni, C. D. Striffler, and R. Weiler, 1981 IEEE Int. Conf. on Plasma Science, Santa Fe, NM (May 18-20, 1981).

8. "Intense Microwave Generation from a Non-Neutral Rotating E-Layer," W. W. Destler, H. Romero, C. D. Striffler, R. L. Weiler, and W. Namkung, J. of Appl. Phys. 52, 2740 (1981).

9. "Stability of a Rotating E-Layer in a Magnetron-Type Waveguide," R. Kulkarni, D. Calderone, and C. D. Striffler, Bull. Am. Phys. Soc. 26, 935 (September 1981).

10. "High-Power Microwave Generation from an Intense Rotating Electron Beam," W. W. Destler, D. Calderone, R. Kulkarni, W. Namkung, R. Weiler, and C. D. Striffler, 1982 IEEE Int. Conf. on Plasma Science, Ottawa, Ontario, CANADA (May 17-19, 1982).

**Abstract Submitted**
**For the Twenty-third Annual Meeting**
**Division of Plasma Physics**
**October 12 to 16, 1981**

**Category Number and Subject** 4.8 Microwave Generation

[X] **Theory** [ ] **Experiment**

Stability of a Rotating E Layer in a Magnetron-Type Waveguide*, R. KULKARNI, D. CALDERONE, and C.D. STRIFFLER, U. Maryland.--Recently, we reported [1] the results of a set of experiments in which the EM radiation was measured from a system containing a rotating E layer propagating along two different outer cylindrical wall structures; one a hollow smooth wall, the other a magnetron-type wall. The main result of these experiments was the enhancement of radiation at a single frequency when a magnetron-type wall was present versus the rather broadband spectrum for the hollow smooth waveguide. We have performed an extensive analysis on the linear EM stability of a thin rotating E layer in a hollow waveguide[2]. Here we present the linear stability analysis for a magnetron-type wall structure. The fields and dispersion relation of the magnetron structure are calculated approximately and the resonant interaction of these normal modes with a beam wave is analyzed.

*This work is supported by AFOSR, the Minta Martin Fund, and the U. Maryland Computer Center

[1] W.W. Destler, R.L. Weiler, and C.D. Striffler, Appl. Phys. Lett. 38, 570 (1981).

[2] W.W. Destler, H. Romero, C.D. Striffler, R.L. Weiler, and W. Namkung, J. Appl. Phys. 52, 2740 (1981).

[X] **Prefer Poster Session**

[ ] **Prefer Oral Session**

[ ] **No Preference**

[ ] **Special Requests for placement of this abstract:**

[ ] **Special Facilities Requested (e.g., movie projector)**

**Submitted by:**

Charles D. Striffler

**(signature of APS member)**

Charles D. Striffler

**(same name typewritten)**

Electrical Engineering Dept.
University of Maryland, College Park, MD 20742

**(address)**

**This form, or a reasonable facsimile, plus *Two Xerox Copies* must be received NO LATER THAN Thursday, July 9, 1981, at the following address:**

**Division of Plasma Physics Annual Meeting**
**c/o Ms. Joan M. Lavis**
**Grumman Aerospace Corporation**
**105 College Road East**
**Princeton, New Jersey 08540**

# 1982 IEEE INTERNATIONAL CONFERENCE ON PLASMA SCIENCE

MAY 17-19, 1982

High-Power Microwave Generation from an Intense Rotating Electron Beam,* W. W. DESTLER, D. CALDERONE, R. KULKARNI, W. NAMKUNG, R. WEILER, and C. D. STRIFFLER, U. Maryland, Electrical Engineering, College Park, MD 20742.

This paper presents the experimental and theoretical results that have been obtained during the past year at the University of Maryland on the production of high-power microwave generation from an intense, relativistic, rotating, annular electron beam. The diode is composed of a knife-edged cathode of radius 6 cm and an anode plate through which the beam passes into a cusped field. The resulting rotating beam interacts with various downstream wall structures; hollow, coaxial and slotted outer or inner wall (magnetron-type). As the beam enters the downstream structure, its properties are nominally 2 MeV, 2 Kamps, and 5-10 nsec pulse width.

In the experiment, the radiation spectrum is examined in X band (8-12 GHz), KU band (12-18 GHz) and KA band (26-40 GHz) as a function of applied cusp magnetic field and waveguide-wall structure. Previous results[1] indicate a broad band spectrum for the hollow and coaxial wall systems with around 1 MW radiated power per mode in X band dropping to around 100 KW in KA band. Previous results[2] for a 12 slot multi-resonator outer boundary indicated about 200 MW of power at 9.6 GHz. Recently we have examined both outer and inner wall slotted structures with strict attention being paid to the various geometric dimensions, slot width and depth. These results will be presented with particular emphasis put on identification of the pertinent wall parameters for efficient beam-waveguide coupling. Besides our previous work[1] in theoretically examining the mechanism of beam-waveguide coupling for a coaxial wall system, we will present an EM linear stability analysis for a slotted wall system, again concentrating on establishing the pertinent wall parameters for efficient coupling.

Recently, we have designed a small version of the above experiment, called CUSPTRON. This design will be presented along with relevant theoretical examination of the beam-waveguide stability. Because of the low beam voltage, it may be necessary to insert an annular dielectric liner in order to slow down the phase velocity of the waveguide modes so that the resonant beam-waveguide interaction can be improved.

1. W. W. Destler, H. Romero, C. D. Striffler, R. L. Weiler, and W. Namkung, J. Appl. Phys. 52, 2740 (1981).

2. W. W. Destler, R. L. Weiler, and C. D. Striffler, Appl. Phys. Lett. 38, 570 (1981).

* Work Supported by AFOSR, Minta Martin Engineering Fund, and U. Maryland Computer Center.

Please refer to "First and Final Call for Papers" announcement for instructions in preparing your abstract.

Subject category name: High-Power Microwave and Sub-Millimeter Wave Generation

Subject category number: 18

( ) Prefer oral session

(X) Prefer poster session

( ) No preference

( ) Special requests for placement of this abstract

Submitted by:

(signature)

Charles D. Striffler
(same name typewritten)

(full address)

I am a member of the Committee on Plasma Science and Application

(X) yes ( ) no

D

FI